A Study of the Handset Antenna and Human Body Interaction

Michal Okoniewski, *Member, IEEE*, and Maria A. Stuchly, *Fellow, IEEE*

(Invited Paper)

Abstract— **The antenna radiation pattern and other characteristics are significantly altered by the presence of the human body. This interaction as well as the resultant deposition of microwave power in the body (specific absorption rate—SAR) are of particular interest for cellular telephones and similar communication devices. This paper builds on and extends the previous analyses of parameters that influence the antenna-user interaction. Computer tomography (CT) and magnetic resonance imaging (MRI)-derived, high-resolution models of the human head are used. The numerical analysis is performed with the finite-difference time-domain (FDTD) method. The specific findings are: 1) a box model of a human head provides grossly distorted and unreliable results for the antenna radiation pattern; 2) a spherical model of the human head provides results that are relatively close to those obtained with a relatively simple, but more realistic, head model; 3) the SAR values obtained with spherical or simplified head models, that do not include the ear, are greater than those for a realistic head model that includes the ear; and 4) a hand holding the handset absorbs significant amount of antenna output power, which can be considerably decreased by modifying the geometry of the handset metal box.**

I. Introduction

With the expansion of current use and anticipated further increases in the use of cellular telephones and other personal communication services (PCS), there have been an interest and considerable research effort devoted to interactions between antennas on handsets and the human body. These activities are motivated by two factors: 1) a need to evaluate deterioration of the antenna performance and to develop better antennas [1], [2]; and 2) a need to evaluate the rates of RF energy deposition, called specific absorption rates (SAR), in order to evaluate potential health effects [3] and compliance with standards, e.g., the U.S. ANSI standard [4].

Previous analyses ranged from those of simple models of the human head such as a homogeneous sphere, e.g., [5] or a homogeneous head shaped volume [6], to heterogeneous, anatomically correct models based on the magnetic resonance imaging (MRI) [1], [2], [7]–[9]. Several studies dealt with a "generic" model of a cellular telephone at approximately 900 MHz consisting of a monopole on a metal box 15 cm long with a cross section of 5 to 6 cm by 1.3 to 2.5 cm [1], [5], [7], [9]. A few commercially available telephones were analyzed, but details of their antenna type and box geometry were not given [8]. A few antenna designs, whose performance is less affected by the human head and which produce lower SAR's in the head, were also numerically modeled [1], [2]. However, even for these antennas radiation patterns are significantly modified, usually in an undesirable way, by the user's hand.

Considerable efforts have also been also devoted to two other activities, namely the use of simplified, so called "canonical" models of the human head for evaluation of SAR's, and an experimental evaluation of SAR's in simplified but anatomically correct models of the head. The canonical models have been developed in Europe as a part of the COST 244 WG3 project [10]. Two main head geometries are a box and a sphere (both either homogeneous or layered). The telephone antennas are modeled as a dipole or a monopole on a metal box. The recent experimental effort is exemplified by work in the United States [11] and Switzerland [12].

In this paper we build on and extend the previous analyses of parameters that influence the interaction between the antenna and the user's body. Specifically, we address the following issues: 1) to what extent the effect of the human head on the antenna radiation pattern can be simulated by a box or a sphere; 2) how well do SAR's obtained with various canonical models predict those in the head; 3) how important are the quality and resolution of the head model in determination of the head effect on the antenna pattern, total power absorbed in the head (or antenna efficiency in the presence of the head), the peak SAR, and the maximum SAR in 1 g and 10 g of tissue; and 4) how does the distance between the antenna and the head affect the values and location of the peak, 1 g and 10 g values of SAR. Additionally, we include the effect of the hand on the parameters investigated and explore a new handset box design that mitigates the effect of the hand on the antenna radiation pattern. Modeling is limited to a realistic position of the handset and its vertical orientation, as tilted orientation results in lower SAR's [1], [7].

II. Models of the Head and Telephone

A. Models of the Human Head and Hand

Three box models of the head were used, each consisting of a 20 cm cube made either of 1) homogeneous brain tissue

Manuscript received November 13, 1996; revised February 22, 1996. This work was supported in part by the Natural Sciences and Engineering Research Council of Canada, BC Hydro, TransAlta Utilities, and TR Labs, Calgary, Alberta.

The authors are with the Department of Electrical and Computer Engineering, University of Victoria, Victoria, BC, Canada, V8W 3P6.

Publisher Item Identifier S 0018-9480(96)07031-7.

TABLE I
DIELECTRIC PROPERTIES OF THE TISSUES USED IN THE HEAD MODELS AT 915 MHz

Tissue	Gent Model [9]		Yale Model [13]	
	ε'	σ (S/m)	ε'	σ (S/m)
skin			35	0.6
skull	8	0.11	8	0.11
spinal cord			49	1.1
spine			8	0.11
brain - white matter	38	0.8	38	0.8
brain - gray matter	49	1.1	49	1.1
jaw bone			8	0.11
muscle	58	1.4	58	1.4
parotid gland			55	1.0
lacrimal glands			55	1.0
spinal canal			72	2.1
tongue			55	1.0
pharynx			35	0.6
esophagus			35	0.6
nasal septum			35	0.6
fat	6	0.08	6	0.08
blood			62	1.5
CSF	78	2.1	78	2.1
eye - sclera	66	1.9	66	1.7
eye - humour			74	2.0
lens			44	0.8
bone marrow			42	0.8
cartilage			35	0.6
pituitary gland			55	1.0
ear bones			35	0.6
trachea			35	0.6

($\varepsilon_r' = 43, \sigma = 0.8$ S/m); 2) single-layered: brain and skull 0.5 cm thick ($\varepsilon_r' = 8, \sigma = 0.11$ S/m); or 3) double-layered: brain, skull 0.5 cm and skin 0.5 cm thick ($\varepsilon_r' = 35, \sigma = 0.6$ S/m). Three similar spherical models were used, each of 20 cm diameter, namely, homogeneous brain, single-layered sphere consisting of brain and skull, and double-layered sphere consisting of skin, skull and brain.

Three anatomically based models of the human head were used. A previously developed and used for modeling of a cellular telephone MRI-based model [9] had a resolution of 3.9 × 3.9 × 5 mm (5 mm in the vertical direction). Two high resolution accurate models were based on CT and MRI scans and were developed at the Radiology Department at Yale University [13]. One high quality model had the resolution 3.4 × 3.4 × 4.7 mm and the other 1.1 × 1.1 × 1.4 mm with many specific tissues and organs identified. We also made some additional improvements to all these models. Table I summarizes the tissues segmented and the dielectric constant and conductivity allocated at 915 MHz to the tissues in these models.

The hand model was highly simplified and comprised only two tissues, bone surrounded by muscle. The bone thickness was 0.5 cm and surrounding muscle was 0.5–2 cm. The hand was wrapped around three sides of the telephone handset.

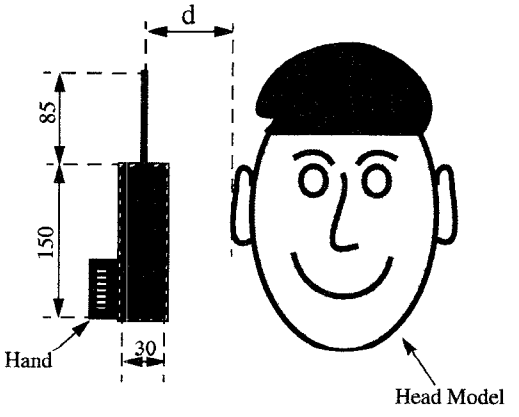

Fig. 1. Geometry of the problem 2.

B. Model of a Cellular Telephone

Since the prevailing design of the 900 MHz cellular telephone today uses a monopole antenna and a nearly rectangular

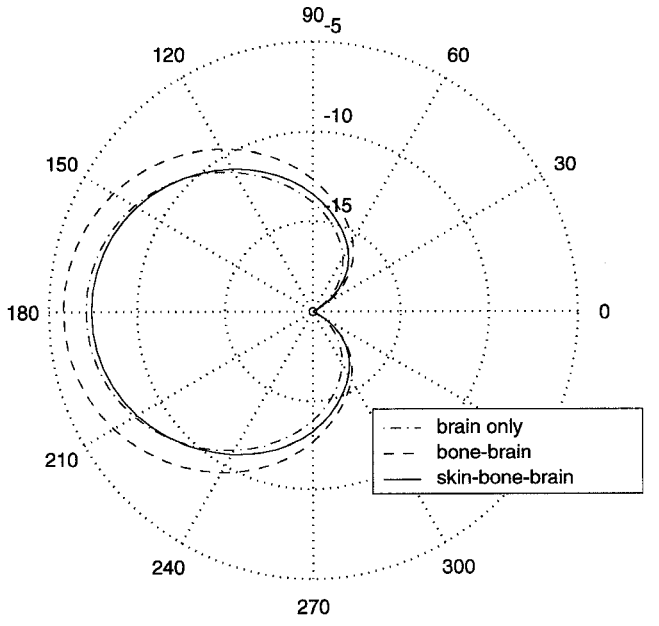

(a)

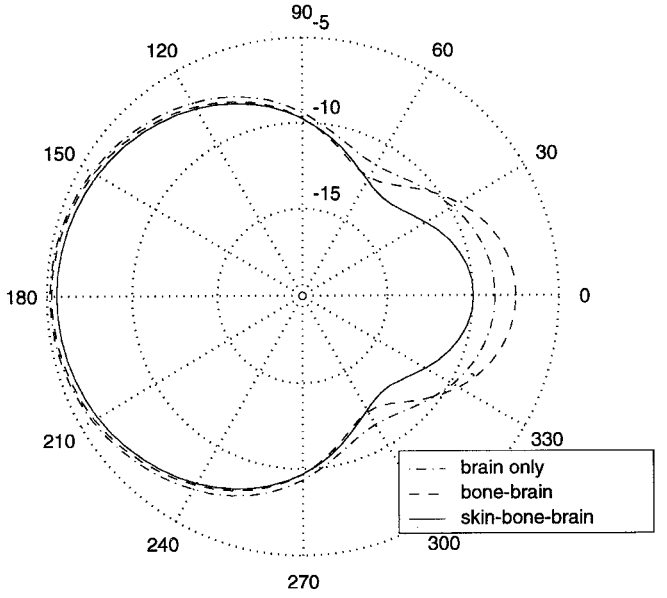

(b)

Fig. 2. Radiation patterns in ϕ-plane for amonopole at 915 MHz on a dielectric covered metal box; distancebetween the antenna and the head model is 1.5 cm, $\theta \simeq 90°$. (a) 20 cm box and (b) 20 cm diameter sphere.

box, the following are dimensions of our model, an antenna length of 8.5 cm, a metal box of 15 (length) × 6 (width) × 3 (depth) cm (Fig. 1). The antenna is centered on the box. The metal box is covered with a dielectric insulator of 2 mm thickness and $\varepsilon_r' = 2.0$.

III. Method of Analysis

The FDTD method was used for the analysis because of its flexibility and efficiency in solving complex heterogeneous geometries. The Yee-cell, rectangular computational grid [14]

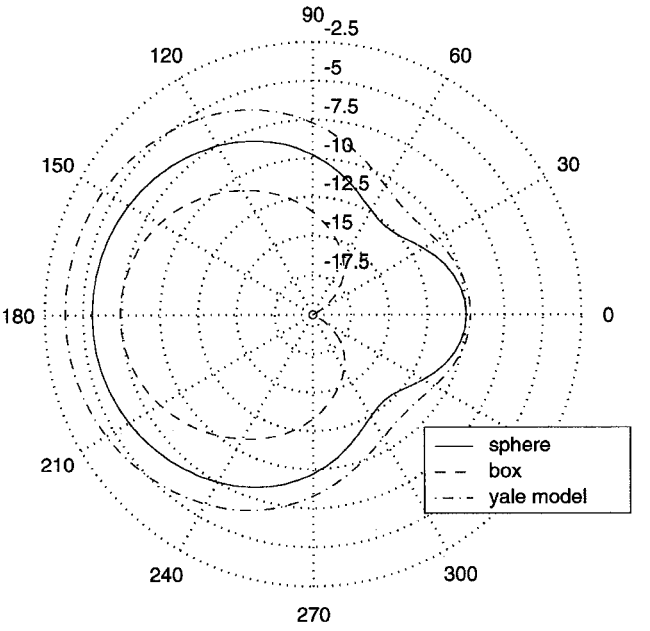

Fig. 3. Radiation patterns in ϕ plane with $\theta \simeq 90°$ for a monopole at 915 MHz on a dielectric covered metal box for a three-layered tissue box and sphere, and a CT-based (Yale) head model.

and the total-field formulation [15] were used. The computational space was truncated by a perfectly matched layer (PML) [16] of 7 cell thickness with a parabolic profile to ensure reflections below at least 40 dB. Two mesh sizes were used; either 5 mm or 3.4 mm, and are given for each case considered. In the analysis with subgridding 1.7 mm mesh was used.

A special automatic algorithm is used to handle dielectric objects with shapes and/or voxels that do not coincide with the FDTD mesh. This algorithm considers the field-continuity conditions and the integral form of Maxwell's equations in a subcell regime. Using fast logic integration the weighted flux averages are computed and look-up tables of the dielectric constant and conductivity are assembled for each field component separately. This algorithm increases the accuracy of computations.

In the cases where the metal surfaces did not coincide with the mesh, an algorithm was used that allows for accurate treatment of fields near these surfaces [17]. To model fields in selected subregions of the head, a subgridding algorithm developed in our laboratory was applied [18]. Computations were performed on a Hewlett-Packard workstation HP9000/735. A typical CPU time for 5×10^5 computational cells including preprocessing was about 60 minutes.

The far-field antenna pattern was obtained from the computed near-field electric and magnetic field vectors on a box enclosing the modeled structures using the field equivalence principle [15]. The antenna efficiency was computed as

$$\eta = \frac{P_{\text{rad}}}{P_{\text{rad}} + P_{\text{abs}}} \tag{1}$$

where P_{rad} was calculated by integrating the normal component of the Poynting vector over the surface of the box used

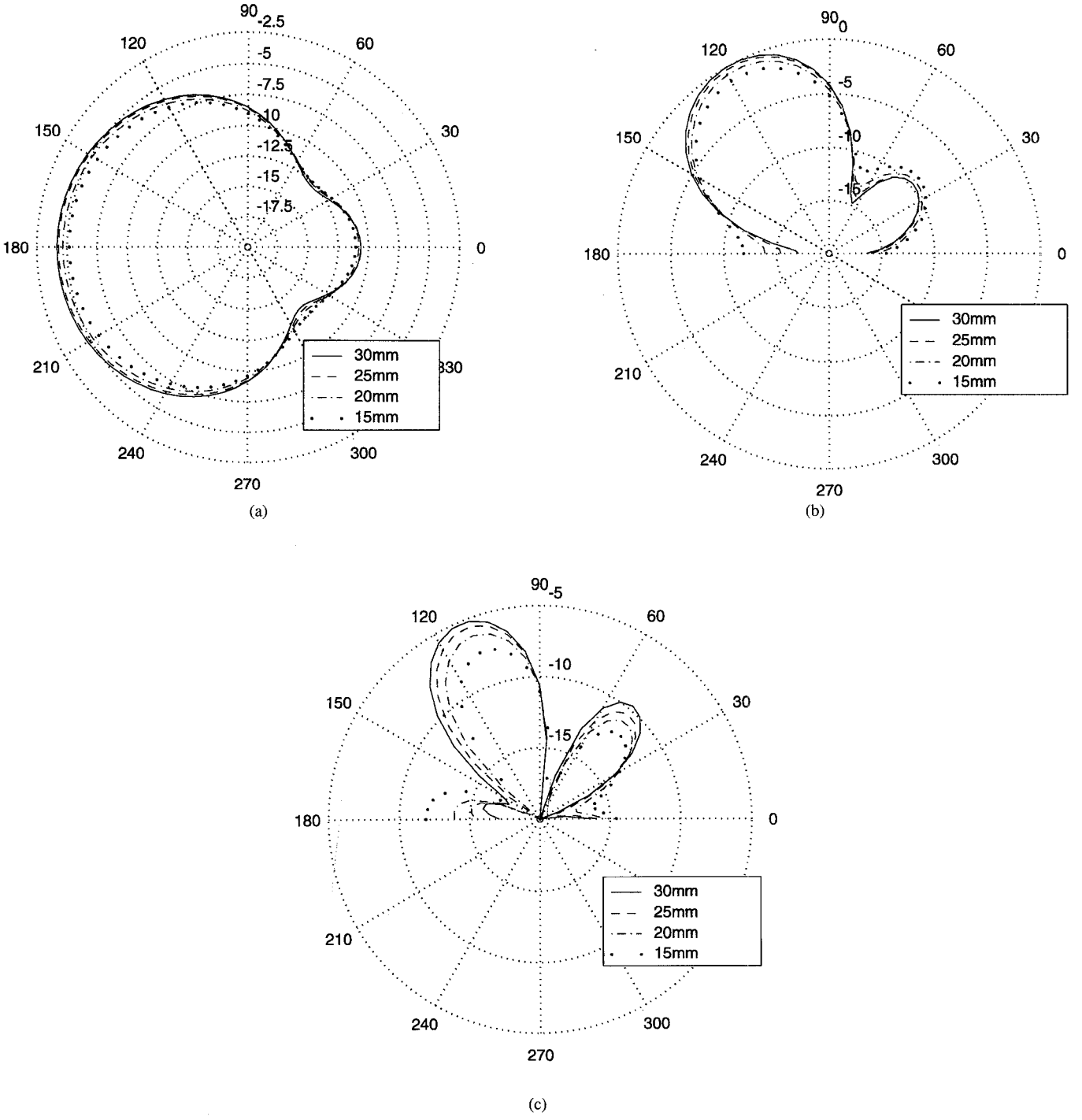

Fig. 4. Radiation pattern for a monopole on a dielectric covered metal box at 915MHz as a function of distance from the head model (no hand). (a) ϕ plane with $\theta = 90°$, (b) θ plane with $\phi = 180°$(away from the head), and (c) θplane with $\phi = 0°$ (toward the head).

for calculations of the near-far-field transformation. The power absorbed (in the head model and hand) was calculated as

$$P_{\text{abs}} = \frac{1}{2}\int_v \sigma |E_t|^2 dv \tag{2}$$

where E_t is the total electric field in a voxel of tissue. The SAR was computed as

$$\text{SAR} = \frac{\sigma}{2\rho}|E_t|^2 \tag{3}$$

where

σ tissue conductivity;

ρ tissue density.

IV. Modeling Results and Discussion

The configuration of the head models and the handset is shown in Fig. 1. It should be noticed that distance d is defined between the monopole and the closest head surface,

TABLE II
COMPARISON OF ANTENNA EFFICIENCY, POWER ABSORBED IN THE HEAD, AND THE SAR'S FOR VARIOUS HEAD MODELS; HAND NOT INCLUDED 1 W, 915 MHz, DISTANCE OF ANTENNA FROM MODEL, 1.5 cm

Head Model		η (%)	P_{abs} (W)	SAR_{peak} (W/kg)	SAR 1g (W/kg)	SAR 10g (W/kg)
Box	homogeneous	16	0.84	18.1	14.1	9.25
	skull-brain	24	0.76	9.6	8.2	5.8
	skin-skull-brain	19	0.81	11.8	8.5	5.5
Sphere	homogeneous	46	0.54	13.4	10.9	7.0
	skull-brain	52	0.48	9.4	8.5	5.5
	skin-skull-brain	45	0.55	8.2	5.4	4.3
Anatomical	Gent Head	51	0.49	11.2	8.6	4.8
	Yale Head - with ear (resolution 5 mm)	60	0.40	3.5	2.7	1.8
	Yale Head - no ear (resolution 5 mm)	50	0.50	6.5	5.4	3.5
	Yale Head - with ear (resolution 3.4 mm)	53	0.47	3.9	2.6	1.8

TABLE III
EFFECTS OF THE HEAD MODEL QUALITY AND HAND, MONOPOLE ANTENNA AT 915 MHz, 1 W, DISTANCE OF ANTENNA FROM HEAD, 3 cm

Head Model	η (%)	P_{abs} (W)	SAR (W/kg)			
			Head Peak	Hand Peak	1g head	10g head
Univ. of Gent; no hand (resolution 5mm)	72	0.28	3.15	-	2.42	1.4
Yale Univ.; no hand (resolution 5mm)	77	0.23	1.7	-	1.1	0.8
Yale Univ.; with hand (resolution 5mm)	61	0.39	-	14	1.5	0.8
Yale Univ.; no hand (resolution 3.4 mm)	75	0.25	4.1	-	1.9	1.4
Yale Univ.; "zoom" (resolution 1.7 mm) no hand	75	0.25	7.9	-	1.9	1.4

the ear, if the model contains it. For all the graphs presenting the results of the computations the following applies: 1) the steady-state radiated power from the antenna is 1 W (i.e., the power radiated in the far field plus the power dissipated in the head and hand where applicable); 2) the antenna patterns are normalized to those obtained for the Yale head model and 3 cm separation between the handset and the head using 5 mm FDTD mesh; and 3) the color three-dimensional (3-D) graphs show the dissipated power density (this quantity is different from the SAR (though proportional to it), as it does not account for the tissue dosimetry) in dB scale normalized to the maximum for a given simulation.

A. Antenna Pattern

Fig. 2 shows the effect of different tissues in the box and spherical models on the antenna pattern in ϕ-plane for $\theta = 90°$. What is apparent from Fig. 1(a), but not surprising, is that the box representing the head nearly entirely blocks the radiation in the head direction. In the case of the sphere [Fig. 1(b)], there is a less dramatic but significant reduction in power radiated toward the half-space where the head is located. The antenna pattern in θ-plane is asymmetric, with the differences between two models of the same character but little (below 2 dB) variability for different tissue models.

A comparison of the antenna pattern for the three models of the head is given in Fig. 3. The effect of the anatomically correct head is overall reasonably well simulated (± 3 dB) by a three-layered sphere. This observation further confirms the finding by Jensen and Rahmat-Samii [1] who used a less anatomically correct model of the head and a different antenna. The differences they computed were somewhat bigger, which is easily explainable by the different antenna geometry (side-mounted PIFA).

TABLE IV
EFFECTS OF THE CHANGE IN THE SEPARATION BETWEEN THE ANTENNA AND THE HEAD MODEL, 915 MHz, 1 W

Model	Separation (cm)	η (%)	P_{abs} (W)	SAR in the head (W/kg)		
				Peak	1 g	10 g
Homogeneous Box	1.5	16	0.84	18.1	14.1	9.25
	2.0	25	0.75	11.2	8.5	5.6
	2.5	40	0 60	5.7	4.3	3.1
	3.0	51	0.49	3.2	2.6	1.9
Homogeneous Sphere	1.5	46	0.54	13.4	10.9	7.0
	2.0	57	0.43	8.5	6.8	4 6
	2.5	66	0.34	5.5	4.4	3.0
	3.0	73	0.27	3.7	3.0	2.1
Gent Head	1.5	51	0.49	11.2	8.6	4.8
	2.0	57	0.43	7.1	5.6	3.3
	3.0	72	0.28	3.2	2.4	1.4
Yale Head	1.5	60	0 40	3.5	2.65	1.8
	2.0	67	0.33	2.4	1.7	1.4
	2.5	73	0.27	1.9	1.2	0.9
	3.0	77	0.23	1.7	1.1	0.8

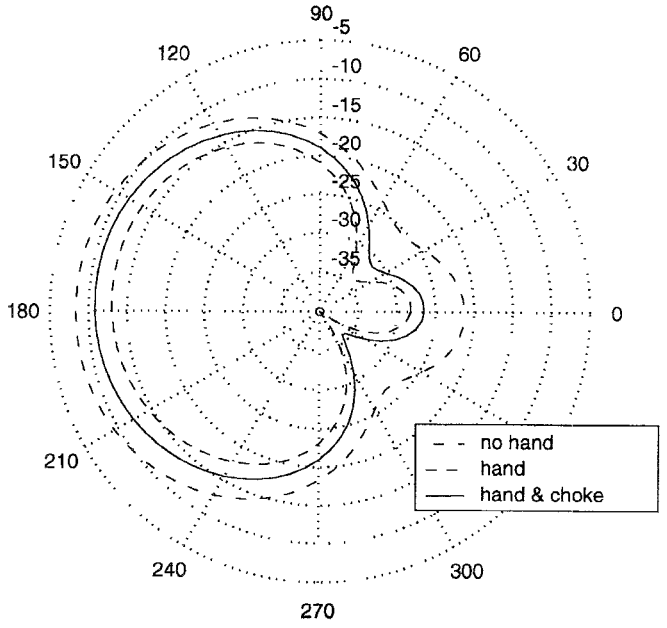

Fig 5. Radiation pattern for a monopole on a dielectric covered metalbox of 915 MHz at 2 cm away from the head model, without the hand, with the hand, and with the hand and a choke

The effect of the distance between the antenna and the user's head is shown in Fig. 4. It can be noted from Fig. 4(a) that in ϕ-plane, as the distance increases the antenna pattern is less affected, but for the small distances considered here, the differences are small. A comparison of the radiation patterns in θ-plane in the half-plane away from the head [Fig. 4(b)] and the half-plane of the head [Fig. 4(c)] shows that, predictably, less power is radiated toward the head direction. Also the angles of nulls have changed from those of a monopole antenna on the box ($\theta = 0$ and $\theta = 180°$).

B. Radiation Efficiency and Power Absorbed

Table II provides summary data to illustrate two issues investigated in this project, namely the utility of the simplified "canonical" models and the significance of quality of a more realistic model of the head. It needs to be noted that with the distance defined as in Fig. 1, the contact between the handset and the model can be physical but not electrical, as the box is insulated with a thin dielectric. The latter is important, as otherwise significantly overestimated SAR's are obtained. The following observations can be made. As previously indicated by the antenna patterns, the box models of the head at close distances to the phone give lower antenna efficiency and higher absorbed power in the head, and consequently higher SAR's, in comparison to other models. Data shown in the Table is for the shortest distance of 1.5 cm (corresponding to the handset in contact with the model). For greater separations, up to 3 cm, a similar influence of the basic model type and tissue composition occurs. Spherical models provide estimates of the antenna efficiency and total absorbed power in the head that are in reasonably good agreement with relatively low resolution head models. One of the critical differences between the Gent and Yale models is the detailed structure of the ear in the Yale models. Data obtained for the Yale head with the ear artificially removed are much closer to those for the spheres and the Gent head.

An important practical conclusion that can be drawn from our data is that spherical (and box) models of the head give overestimated values of the decrease in the antenna efficiency as well as of the total power absorbed and various local and limited volume averaged SAR's.

An additional illustration of the effect of an improved model resolution on the antenna efficiency and SAR's is given in Table III. The same Yale head modeled with 5 mm and 3.4 mm

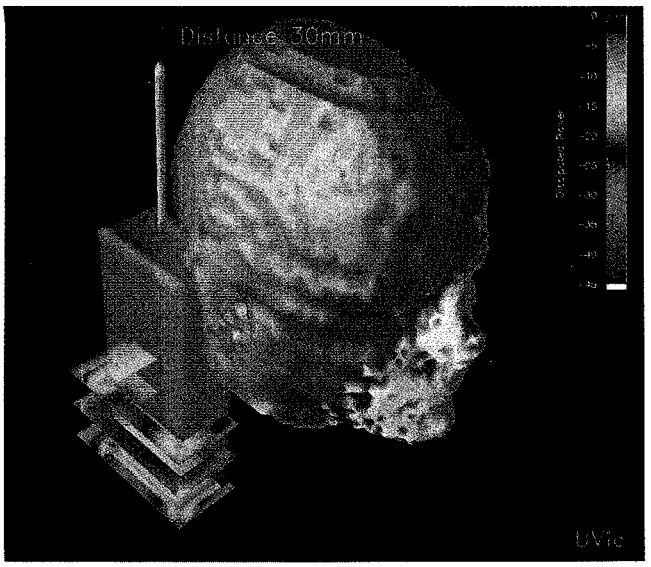

Fig. 6. SAR distribution in various cross sections of the hand and on the surface of the head; antenna–head separation 2 cm.

Fig. 7. SAR distributions in the Yale head (with ear) model at 915 MHz; hand not included, antenna–head separation 1.5 cm, results normalized to the peak SAR.

FDTD meshes shows higher SAR's for the 3.4 mm resolution, while the antenna efficiency and total power absorbed are only slightly different. In the case of the subgridding (zoom), a part of the head adjacent to the handset is modeled with twice the resolution of the remaining head, i.e., 1.7 mm. It can be noted that in the case of the zoom the peak SAR is higher, which is to be expected as it refers to a smaller voxel.

C. Effect of the Hand Holding a Handset

Table III highlights how the hand holding a handset that is made of metal covered with a thin loss-less dielectric decreases the radiated power due to the power absorption in the hand. Fig. 5 illustrates the effect on the antenna pattern in ϕ-plane, and Fig. 6 shows the pattern of the SAR. SAR's are shown in various cross sections of the hand, clearly indicating maximal values close the box corners. SAR's are also mapped on the surface of the head. These observations regarding the power absorption in the hand further confirm earlier reports [1], [8].

We have also experimented with interrupting the current flow on the box and limiting it to the surface not normally in contact with the hand to determine if it can limit or eliminate the problem. A simple unoptimized choke that provides an apparent open circuit on the upper surface of the antenna box improves the antenna efficiency from 61% to 70% compared to 77% without the hand (separation of 3 cm between the antenna and the head). Correspondingly, the peak SAR in the hand decreases to 5.8 W/kg from 14 W/kg. The effect of the choke on the antenna pattern is shown in Fig. 5.

D. Antenna–Head Separation

Changes in the antenna efficiency, power deposited and SAR's with separation between the antenna and various models of the head are summarized in Table IV. It is worth noting, that the box head model is not adequate even for larger separations. The similarities, in terms of the results obtained, between the spherical model and the simpler head model without an ear remain even for greater separations. A comparison between the Gent and Yale heads on the basis of the obtained data in Table IV suggests that separations 3.0 and 1.5 cm, respectively are equivalent. This observation is further supported by an approximate separation due to the ear (thickness of ear), as explained earlier in our definition of distance.

Our results are in good agreement with those reported elsewhere for both the antenna efficiency [1] and the SAR in 1 g of tissue [1], [2]. A reduction by a factor of nearly 2 in the SAR occurs for an increase in the separation by 1 cm, but the decrease is not inversely proportional to the square of distance.

E. SAR Patterns

Fig. 7 shows the distribution of the peak SAR in the head in two planes for the Yale model with 1.5 cm distance from the monopole antenna, the hand is not included. The planes are selected to show the maximum value of the SAR. The horizontal plane is in the plane of the antenna feed and the upper plate of the handset box. The vertical plane passes through the back portion of the ear. The maximal peak SAR occurs in the skin behind the ear, and maximal 1 g and 10 g SAR's are in the skin and skull tissue. Further illustration of the peak SAR distribution is given in Fig. 8 which shows SAR values in the surface layer of the skull and the brain. The values shown are normalized to the maximum that is in the skin and therefore not shown on these graphs. It is worth

Fig. 8. SAR distributions on the surface of the skull and the brain cortex for the Yale head (with ear) model at 915 MHz; hand not included, separation 1.5 cm, results normalized to the peak SAR (the same as in Fig. 6).

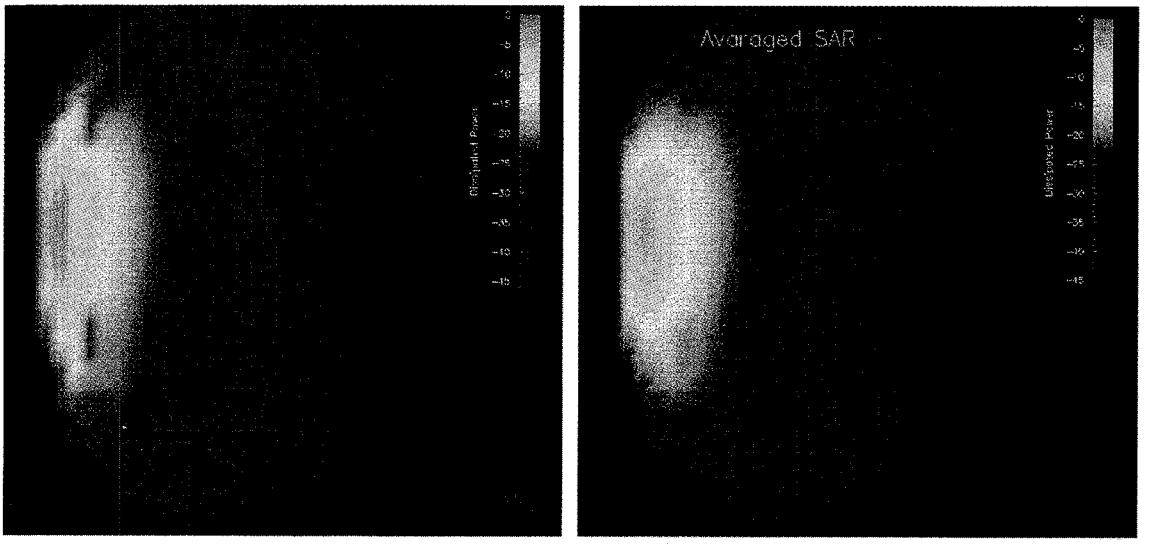

(a) (b)

Fig. 9. SAR distribution in a cross section that includes the maximum. (a) Peak and (b) average over 1 g.

noticing that in the surface layer of the brain cortex the peak SAR's are relatively close to those in the skull for a limited area. Fig. 9 shows the distribution of SAR in the plane of the maximum SAR (SAR on the brain surface shown in Fig. 8).

F. Fine Mesh Analysis

Subgridding technique may be effectively used to increase the resolution where necessary. Fig. 10 shows the SAR distribution on the brain surface. The inset illustrates the region where the density of the mesh was increased by a factor of 2. Higher resolution generally increases peak SAR observed, in this case by approximately 3 dB. Note however, that in the case of subgridded mesh, voxel size, where SAR is observed, is decreased by a factor of 8. It is worth noting, that had the entire mesh density been increased by a factor of 2, 8 times more memory and 16 times more CPU time would have been required. In this example, the overall increase of computer resources required was 80%.

V. Conclusion

The FDTD technique with modern features such as Berenger's absorbing boundaries [16], an accurate dielectric properties averaging algorithm, an accurate modeling of perfectly conducting surfaces that do not coincide with the mesh [17] and a subgridding algorithm facilitate effective computations for modeling interactions of cellular telephones with the human head. Extensive data examining various issues have been obtained. Moderate computation times, of

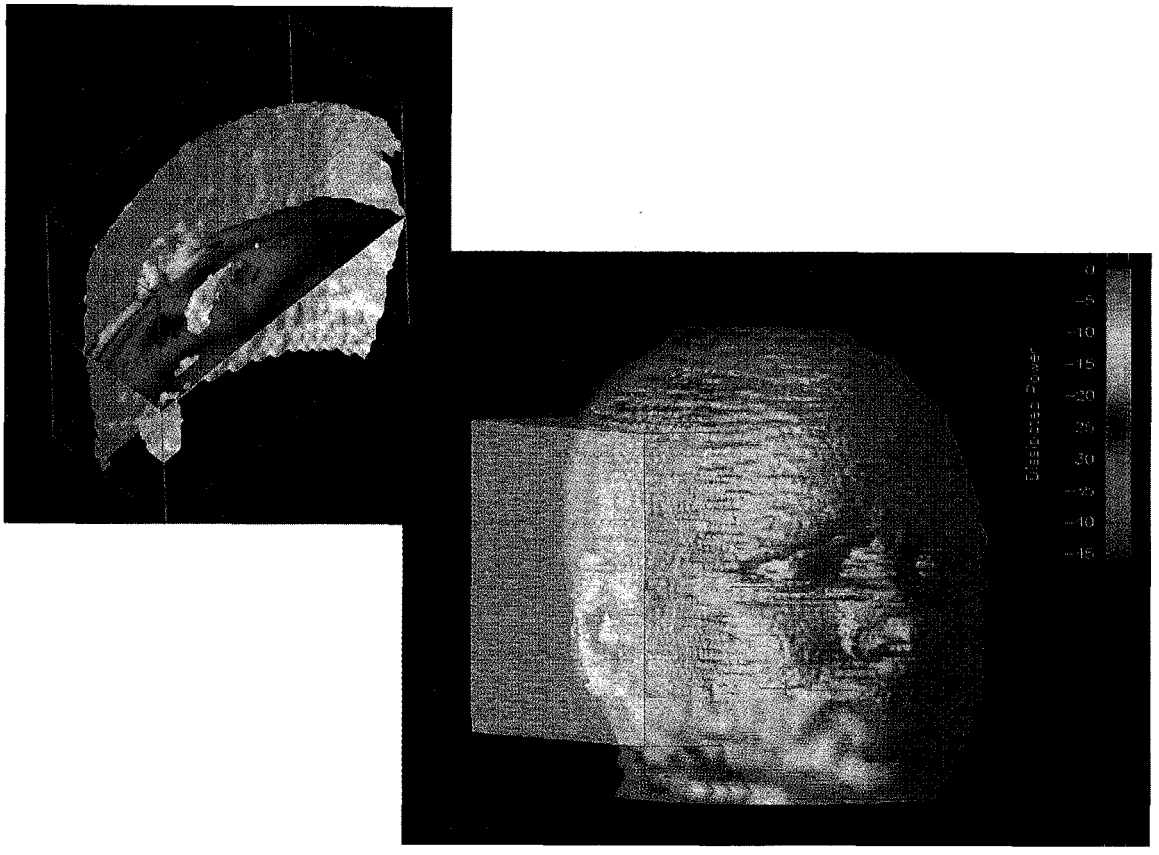

Fig. 10. SAR distribution. Yalehead, separations 3 cm. The insert presents result obtain edusing subgridding technique. Both graphs are in the same scale.

the order of one hour are required on a typical workstation (HP 9000/735). The various values of SAR reported in this work and by others (particularly [1], [7], and [8]) are useful in determining compliance of cellular phones with various recommendations concerning health effects of RF/microwave radiation. However, caution should be exercised regarding the accuracy of the specific SAR values reported in this work (and perhaps others). Since the details of the head anatomy, position of the antenna on the box, and with respect to the head and geometry of the box (handset) play a role, we estimate our confidence in the results to be within 10%. Since the antenna pattern is to a lesser degree affected by the quality of the head model and other geometrical factors, the data are perhaps more reliable, however from the practical viewpoint differences of the order of 1 dB are not critical.

A practical conclusion that can be drawn from this work is that a spherical head model, while not accurate, provides easy and reasonably effective means for the estimation of the "worst case SAR" either through modeling or experiment. Data reported by us, as well as data previously published, support the statement that it is highly unlikely that higher SAR's averaged over 1 or 10 g of tissue are produced in actual human heads than those obtained for the spherical model. As shown, all SAR's (peak, 1 g, 10 g) are lower for an anatomically correct model of the human head.

It is important to include the hand in evaluating the antenna performance and SAR's in the head. The hand absorbs a significant amount of the antenna output power and therefore detrimentally affects the performance of the telephone. However, its presence decreases rather than increases SAR's in the head. The absorption of power in the hand can be decreased or perhaps even eliminated. A reduction of the power absorbed by the hand by over 50% can be accomplished by a relatively simple choke.

ACKNOWLEDGMENT

The authors appreciate the generous sharing of the CT and MRI head models by G. Zubal of the Department of Diagnostic Radiology, Yale School of Medicine. They also thank L. Martens of the University of Gent for the MRI derived head model.

REFERENCES

[1] M. A. Jensen and Y. Rahmat-Samii, "EM interaction of handset antennas and a human in personal communications," *Proc. IEEE*, vol. 83, pp. 7–17, 1995.

[2] M. A. Douglas, M. Okoniewski, and M. A. Stuchly, "Modeling of wireless personal communication transmitters in the presence of the user's body," *Wireless '95—7th. Int. Conf. Wireless Communicat.*, Calgary, Alberta, July 1995, pp. 77–83.

[3] M. A. Stuchly, "Wireless communications and the safety of the user," *Int. J. Wireless Information*, vol. 1, pp. 223–228, 1994.

[4] ANSI C95.1-1992, "American National Standard safety levels with respect to human exposure to radio frequency electromagnetic fields, 300 kHz to 100 GHz," New York: IEEE, 1991.
[5] J. Toftgard, S. Hornsleth, and J. Bach Andersen, "Effects on portable antennas of the presence of a person," *IEEE Trans. Antennas Propagat.*, vol. 41, pp. 739–746, 1993.
[6] H. R. Chuang, "Human operator coupling effects on radiation characteristics of a portable communication dipole antenna," *IEEE Trans. Antennas Propagat.*, vol. 42, pp. 556–560, 1994.
[7] P. J. Dimbylow and S. M. Mann, "SAR calculations in an anatomically realistic model of the head for mobile communication transceivers at 900 MHz and 1.8 GHz," *Phys. Med. Biol.*, vol. 39, pp. 1537–1553, 1994.
[8] O. P. Gandhi, "Some numerical methods for dosimetry: Extremely low frequencies to microwave frequencies," *Radio Sci.*, vol. 30, pp. 161–177, 1995.
[9] L. Martens, J. De Moerloose, and D. De Zutter, "Calculation of the electromagnetic fields induced in the head of an operator of a cordless telephone," *Radio Sci.*, vol. 30, pp. 283–290, 1995.
[10] L. Martens, "Canonical problems proposed within the framework of the European COST 244 project for comparison of numerical methods used for electromagnetic calculations for mobile communications," in *Proc. PIERS*, Seattle, WA, July 24–28, 1995, p. 691.
[11] Q. Balzano, O. Garay, and T. J. Manning Jr., "Electromagnetic energy exposure of simulated users of portable cellular telephones," *IEEE Trans. Veh. Technol.*, vol. 44, pp. 390–403, 1995.
[12] T. Schmid, O. Egger, and N. Kuster, "Automated E-field scanning system for dosimetric assessments," *IEEE Trans. Microwave Theory Tech.*, to appear 1996.
[13] I. G. Zubal, C. R. Harrell, E. O. Smith, Z. Rattner, G. R. Gindi, and P. H. Hoffer, "Computerized three-dimensional segmented human anatomy," *Med. Phys. Biol.*, vol. 21, pp. 299–302, 1994.
[14] K. S. Yee, "Numerical solution of initial boundary value problems involving Maxwell's equations in isotropic media," *IEEE Trans. Antennas Propagat.*, vol. 14, pp. 302–307, 1966.
[15] A. Taflove, *Computational Electrodynamics: The Finite-Difference Time-Domain Method.* Artech House, 1995.
[16] J.-P. Berenger, "A perfectly matched layer for the absorption of electromagnetic waves," *J. Comp. Phys.*, vol. 114, pp. 185–200, 1994.
[17] J. Anderson, M. Okoniewski, and S. S. Stuchly, "Practical 3-D contour/staircase treatment of metals in FDTD," *IEEE Microwave Guided Wave Lett.*, vol. 6, no. 3, pp. 146–148, Mar. 1996.
[18] M. Okoniewski, E. Okoniewska, and M. A. Stuchly, "3-D sub-gridding algorithm for FDTD," in *IEEE Antennas Propagat. Int. Symp.*, 1995, vol. 1, pp. 232–235.

Michal Okoniewski (SM'86–M'89) was born in Gdansk, Poland, in 1960. He received the M.S.E.E. and Ph.D. (with Honors) degrees from the Technical University of Gdansk, Gdansk, Poland in 1984 and 1990, respectively.

From 1984 to 1986 he was with the Polish Academy of Sciences, and since 1986 with the Technical University of Gdansk as an Assistant Professor. From 1992 to 1994 he was with the University of Victoria, British Columbia, Canada as an NSERC International Postdoctoral Fellow. He is now with the University of Victoria as an Adjunct Professor. His current research interest include FDTD and other numerical methods in electromagnetics, interactions of electromagnetic waves with complex media, guided waves, ferrite devices, microwave hyperthermia and sensors for industrial applications.

Maria A. Stuchly (M'71–SM'76–F'91) received the M.Sc. in electrical engineering in 1962 from Warsaw Technical University and the Ph.D. degree in electrical engineering from the Polish Academy of Sciences in 1970.

Between the years of 1962 and 1970, she was with the Warsaw Technical University, an Institute of the Polish Academy of Sciences. After immigrating to Canada during 1970, her first position was with the University of Manitoba. In 1976, she was employed by the Bureau of Radiation and Medical Devices in Health and Welfare Canada as a Research Scientist. During 1978, she became associated with the Electrical Engineering Department at the University of Ottawa as an Adjunct Professor, and in 1990–1991 as a Funding Director of the Institute of Medical Engineering. In 1992, she joined the University of Victoria as a Visiting Professor with the Department of Electrical and Computer Engineering, and since January 1994 she has been a Professor and Industrial Research Chairholder funded by the Natural Sciences and Engineering Research Council of Canada, BC HYDRO, and Trans Alta Utilities.

Dr. Stuchly was president of the Bioelectromagnetic Society, and the Chairman of the International URSI Commission K "Electromagnetics in Biology and Medicine" from 1991–1993.